ELSEVIER

Materials Science and Engineering A317 (2001) 85–92

MATERIALS SCIENCE & ENGINEERING A

www.elsevier.com/locate/msea

# On the mechanical behavior of single crystal NiTi shape memory alloys and related polycrystalline phenomenon

Ken Gall [a], Huseyin Sehitoglu [b,*], Rob Anderson [b], Ibrahim Karaman [b], Yuriy I. Chumlyakov [c], Irina V. Kireeva [c]

[a] *Department of Mechanical Engineering, University of Colorado, Boulder, CO 80309, USA*

[b] *Department of Mechanical and Industrial Engineering, 140 Mech. Eng. Bldg, University of Illinois, MC-244, 1206 West Green Street, Urbana, IL 61801, USA*

[c] *Physics of Plasticity and Strength of Materials Laboratory, Siberian Physical and Technical Institute, 634050 Tomsk, Russia*

**Abstract**

Room temperature monotonic and cyclic stress–strain curves for single crystal and polycrystalline NiTi shape memory alloys containing $Ti_3Ni_4$ precipitates are presented. The tensile and compressive single crystal results illustrate the importance of crystallographic texture, the unidirectional nature of the martensitic transformation, and martensite detwinning on tension-compression stress–strain asymmetry in polycrystalline NiTi. Moreover, results on the fatigue of NiTi single crystals demonstrate the fundamental characteristics of cyclic deformation in NiTi alloys and the importance of texture on the fatigue of polycrystalline NiTi. 

*Keywords:* Cyclic loading; Detwinning; NiTi single crystal; Shape memory alloy; Stress–strain asymmetry

## 1. Introduction

At the microscopic level, the distinct mechanical properties of shape memory alloys are produced by a reversible thermo-elastic martensitic transformation [1]. Of the dozen or more [2] intermetallic alloys that undergo a thermo-elastic martensitic transformation, equiatomic NiTi alloys have the greatest promise for wide-scale applications due to their exceptional physical and mechanical properties [2]. Owing to intense research efforts around the world, the mechanisms of deformation are well-characterized in polycrystalline NiTi shape memory alloys subjected to *monotonic tensile loading conditions*. However, the characteristics of deformation in polycrystalline NiTi subjected to compression [3] and cyclic loading conditions [4] deviate significantly from the well-documented monotonic tensile response. In polycrystalline NiTi materials deformed under monotonic compression, the critical transformation stress level is higher, the transformation stress–strain slope is steeper, and the recoverable strain levels are smaller compared with tensile results [3]. Furthermore, during mechanical cycling, the stress–strain response of polycrystalline NiTi demonstrates a lowering of the critical transformation stress level, an increase in the transformation stress–strain slope, and a decrease in the transformation hysteresis compared with the first loading cycle [4].

More recent experimental efforts have confirmed the tension-compression asymmetry [5–12] and cyclic effects [9,13–21] in polycrystalline NiTi for a wide range of NiTi alloys and testing conditions. Despite the documented influence of the loading direction and cyclic loading conditions on the deformation of NiTi alloys, many recent constitutive models (phenomenological and micro-mechanical) do not contain the framework to accurately capture the pertinent stress-state and cyclic loading effects. The current deficiencies in shape memory alloy constitutive models are rooted in a poor comprehension of the dominant mechanisms contributing to tension-compression asymmetry and fatigue effects in NiTi alloys. Many earlier studies have focused on the macroscopic deformation characteristics in polycrystalline NiTi or the local mechanisms of deformation

* Corresponding author. Tel.: +1-217-3331176; fax: +1-217-2446534.

*E-mail address:* huseyin@uiuc.edu (H. Sehitoglu).

0921-5093/01/$ - see front matter 
PII: S0921-5093(01)01183-2

Table 1
Transformation temperatures for the Ti–50.8at.% Ni materials in two different aged states[a]

| | $M_s$ (K) | $M_f$ (K) | $R_s$ (K) | $R_f$ (K) | $A_s$ (K) | $A_f$ (K) |
|---|---|---|---|---|---|---|
| Aged 1.5 h at a temperature of 823 K | 231 | 214 | 266 | 251 | 266 | 280 |
| Aged 15.0 h at the rate of 773 K | 270 | 253 | 285 | 274 | 300 | 320 |

[a] The materials were solutionized before aging.

at the electron microscope size scale. However, the unique stress–strain behavior of NiTi polycrystals is also strongly dependent on phenomena best represented at the single crystal (grain) size scale.

Until recently [12,21–24], experimental results on single crystal NiTi shape memory alloys were absent from the literature with exception to one study on the tensile deformation of NiTi single crystals [25]. Without experimental results on single crystal NiTi, it is difficult to understand the deformation behavior of NiTi polycrystals, particularly since the processing of such polycrystals leads to extremely strong crystallographic textures [11,26,27]. To further complicate the physical understandings in polycrystalline NiTi, alloys with compositions that deviate a few percent from equiatomic NiTi may contain precipitates that are unable to undergo the martensitic phase transformation. Elastically deforming second phase precipitates modify the martensitic transformation in the surrounding B2 parent phase, and often invalidate the phenomenological theory of martensitic transformations [22,23]. Without theoretical models for the martensitic transformation in precipitated NiTi, it is difficult to understand and predict the behavior of precipitated textured polycrystals, thus making single crystal experimental results particularly useful. Hence, in this work, we provide a basis for understanding the origins of tension–compression asymmetry and cyclic effects in polycrystalline NiTi shape memory alloys using unique single crystal experimental results.

## 2. Experimental techniques

Polycrystalline NiTi samples were electro-discharge machined from 25.4 mm diameter Ti–50.8at.% Ni cylindrical bars (grain size ~20 μm). Bars from the same material batch were melted and grown into single crystal NiTi ingots using the modified Bridgman technique. Single crystal samples with orientations of [110], [111], and [211] were electro-discharge machined from the bulk single crystal ingot. The tensile specimens were flat dog-bone shaped samples with a 25 mm length and a 3 mm × 1 mm gage cross section. The compressive specimens were rectangular shaped samples with a 7 mm length and a 4 mm × 4 mm cross section. Machined single crystal and polycrystalline specimens were solutionized by holding at 1273 K for 2 h followed by water quenching. The solutionized single crystals of the [110] and [111] orientations and the polycrystalline NiTi were subsequently averaged 15.0 h at the rate of 773 K, yielding 1.0 μm $Ti_3Ni_4$ incoherent precipitates. The solutionized single crystals of the [211] orientation were subsequently averaged 1.5 h at the rate of 823 K, yielding 0.4 μm $Ti_3Ni_4$ incoherent precipitates. The transformation temperatures of the NiTi materials given the two aging treatments are summarized in Table 1. Room temperature monotonic and cyclic mechanical tests were conducted in strain control with an approximate local strain rate of $10^{-4}$ 1 $s^{-1}$, as measured with an extensometer.

## 3. Idealized single crystal response

Fig. 1 is a schematic of the idealized behavior of a single crystal of NiTi undergoing a stress-induced martensitic transformation. At low stress levels, the B2 parent phase deforms elastically (a). At a critical stress

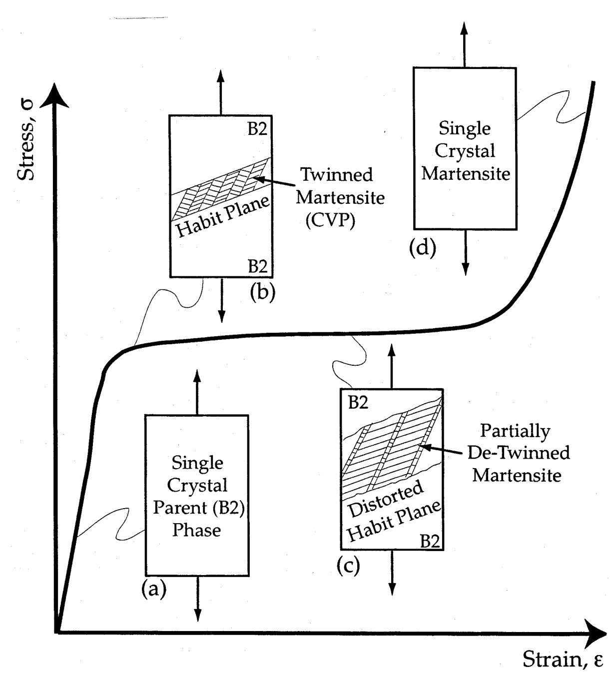


Fig. 1. Schematic demonstrating the stages of the stress-induced martensitic transformation in single crystal NiTi. A correspondence variant pair (CVP) is the same as a martensite plate.

level (b), the martensitic transformation is triggered by a resolved shear stress acting across the most favorably oriented martensite habit plane. Based on the phenomenological theory of martensitic transformations [1], the martensite that forms through a shear across the habit plane has an internally twinned structure. Such a martensite plate can be called a correspondence variant pair (CVP) since two twin related martensite single crystal variants develop. It may be asserted that the martensite is a single crystal even at the onset of the transformation. However, for example, the stress–strain response of NiTi single crystals oriented along the [110] direction indicates that the internally twinned structure is a precursor to a detwinned or single crystal structure (Section 5). After a finite volume fraction of martensite has transformed, the internally twinned martensite may detwin (Fig. 5), as observed within deformed polycrystalline NiTi grains [27]. As the martensite detwins, uniaxial strains are accumulated due to the growth of the favorably oriented single crystal of martensite at the expense of its twin related neighbor.

During the detwinning process, the habit plane (invariant plane) distorts since the evolving volume fractions of twin related single crystal martensites are no longer capable of satisfying the phenomenological theory for NiTi martensites [28,29]. The elastic strain energy caused by the distortion of the habit plane during detwinning, and the friction of interfacial twin boundary motion, are the primary barriers to the detwinning process. The local distortion of the habit plane during the stress-induced transformation has been observed in single crystal shape memory alloys using Morie interference patterns [30]. The aforementioned study [30] concluded that the distortion of the habit plane was caused by the formation of martensite on the habit plane followed by subsequent detwinning during deformation. If the detwinning process reaches 100% completion, then the single crystal of NiTi martensite will deform elastically (d). The idealized behavior described above is complicated by the presence of coherent or semi-coherent $Ti_3Ni_4$ precipitates (0.01–0.30 μm), which can alter the internally twinned state [31,32] and also inhibit detwinning [12].

## 4. Unidirectional Schmid law

In NiTi shape memory alloys, 24 martensite plate variants (CVP's) exist in the B2 parent phase [33–37]. When a single crystal of NiTi is subjected to an external stress, the CVP with the largest resolved shear stress on its martensite habit plane and along its transformation shear direction initiates the transformation. The transformation direction has normal and shear components with respect to the habit plane, however, the shear component dominates the transformation due to the small volume change in NiTi shape memory alloys [35]. A resolved shear stress may exist along the prescribed transformation shear direction, or in the conjugate shear direction. However, due to the crystallography of the martensitic transformation, the transformation will only initiate, if the resolved shear stress is in the same direction as the prescribed transformation direction. Thus, a unidirectional Schmid law is required to describe the critical transformation behavior of NiTi single crystals. In the presence of coherent or semi-coherent $Ti_3Ni_4$ precipitates (0.01–0.30 μm), the Schmid law does not accurately predict the initial transformation behavior of NiTi single crystals without accounting for internal coherency stress fields [12,22,23].

The unidirectional nature of the martensitic transformation creates a considerable orientation dependence and tension-compression asymmetry of the critical stress required to trigger the transformation in single crystals of NiTi as experimentally demonstrated [12,22,23] and predicted by models [35,36,38,39]. Therefore, if polycrystalline NiTi contains a strong crystallographic texture, the polycrystal may demonstrate tension–compression asymmetry. Fig. 2 contains reconstructed [110], [111], and [211] pole figures created from texture measurements on typical drawn bar-stock polycrystalline NiTi. The pole figures in Fig. 2 indicate that the predominant texture along the loading direction (the center of the pole figure) is the ⟨111⟩{110} type. Consequently, if the observed tension-compression asymmetry of the critical transformation stress level in polycrystalline NiTi [3,5–12] is from texture, then deformation characteristics of the textured polycrystalline NiTi should somewhat resemble the deformation characteristics of single crystals oriented along the [111] direction.

Fig. 3 presents tensile (a) and compressive (b) stress–strain curves for the textured polycrystalline NiTi represented in Fig. 2, and single crystals of NiTi oriented along the [111] direction. According to Table 1, the test temperature (295 K) is between the austenite and martensite start temperatures (300 and 270 K, respectively) for this aging treatment, thus the permanent strains in Fig. 3 were only recoverable after heating above the austenite finish temperature (320 K). The single crystal and polycrystalline NiTi materials demonstrate a strong similarity in the overall stress–strain response and the critical transformation stress levels. The stress–strain response for all specimens was found to be reproducible (2 or 3 equivalent tests were conducted). Over multiple tests, the [111] single crystal and polycrystalline NiTi both demonstrate lower critical transformation stress levels under tension compared with their respective compressive responses. The Schmid factors for the transformation in tension versus compression for the [111] orientation are 0.39 and 0.27,

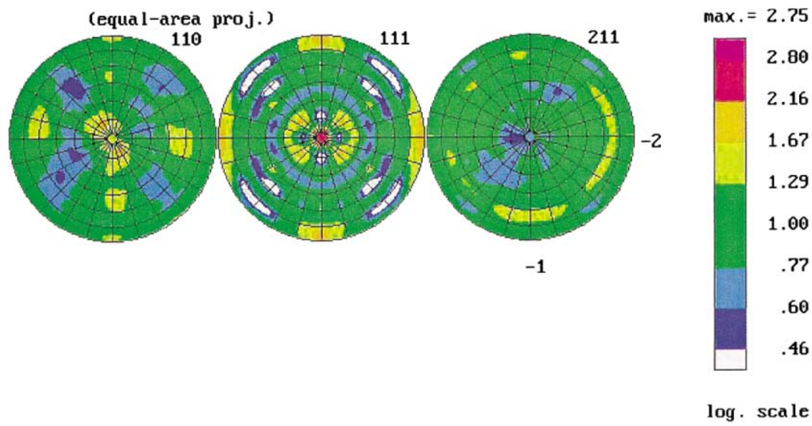


Fig. 2. Measured pole figures indicating the strong texture in drawn polycrystalline NiTi. The loading and drawing axis is at the center of the pole figures.

respectively [12,35], which is consistent with the experimental observations (Fig. 3). The similarity between the single crystal and textured polycrystalline response demonstrate that crystallographic texture accounts for the difference in the tensile and compressive stress–strain responses for polycrystalline NiTi. We have furthered this argument in polycrystalline NiTi by employing a distinctly different approach using single crystal constitutive relationships, a self-consistent averaging scheme, and discretized texture measurements [11].

## 5. Detwinning

In Fig. 3, the recoverable strain levels under tension (a) are significantly larger than under compression (b). Moreover, owing to the similarity between the stress–strain response of the [111] single crystals and the ⟨111⟩{110} textured polycrystals, Fig. 3 demonstrates that the tension-compression asymmetry of recoverable strain levels in NiTi polycrystals originates at the single crystal level. The reason why single crystals of NiTi demonstrate an experimental tension–compression asymmetry of the recoverable strain levels is due to differences in CVP formation and CVP detwinning strains (Fig. 1). However, we observe that CVP detwinning provides a stronger contribution to the difference in recoverable strain levels under tension versus compression. For instance, regardless of the crystallographic orientations of the NiTi single crystal, the detwinning strain (for a {−0.072, 1, 1}⟨0, 1, −1⟩ Type II twin structure) is always smaller under compression versus tension [37].

In Fig. 3 the [111] crystal is oriented to develop 5.1% strain due to CVP formation (the local shear magnitude of 0.13 times the Schmid factor of 0.39), and 3.5% strain due to CVP detwinning under tension [37]. Conversely, under compression, the [111] crystal is oriented to develop 3.5% strain due to CVP formation (the local shear magnitude of 0.13 times the Schmid factor of 0.27), and 0.3% strain due to CVP detwinning [37]. Thus, under compression, the [111] crystal (and the similar polycrystal) is not oriented to develop signifi-

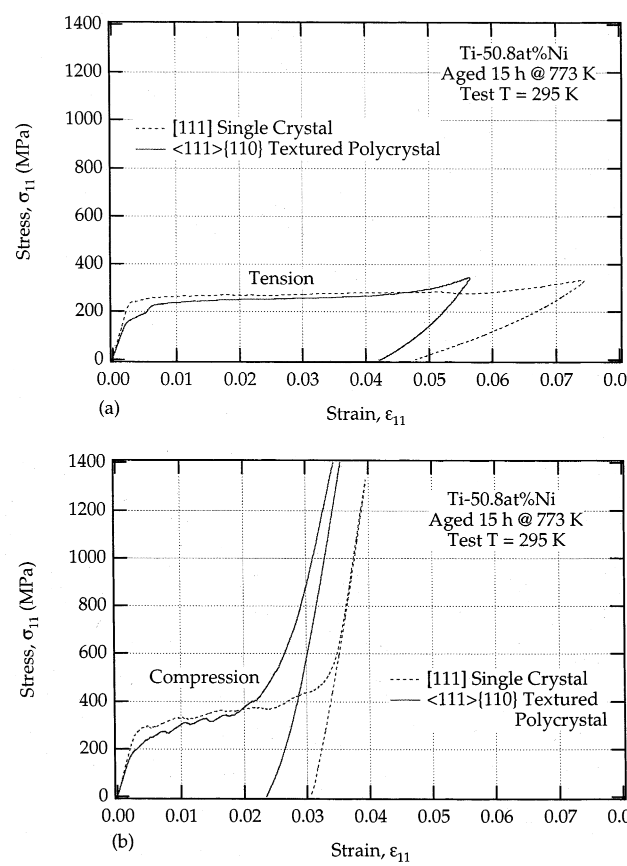


Fig. 3. Comparison of the (a) tensile and (b) compressive stress–strain response of ⟨111⟩{110} textured polycrystalline NiTi and a single crystal of NiTi oriented in the [111] direction. The polycrystalline response continues up to 1500 MPa before load reversal.

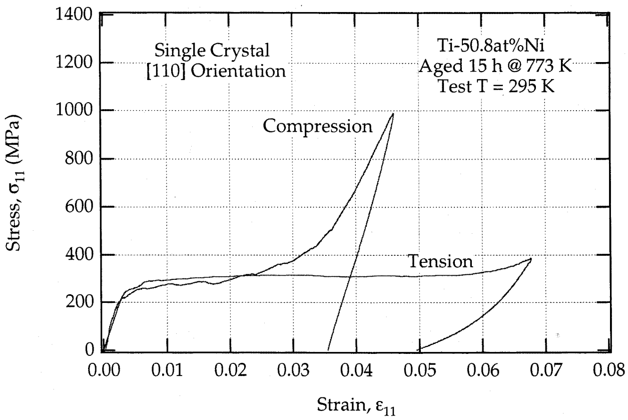


Fig. 4. Tensile and compressive stress–strain response of a single crystal of NiTi oriented in the [110] direction. The test temperature is in between the $M_s$ and $A_s$ transformation temperatures.

cant uniaxial strains due to CVP formation or CVP detwinning compared with tension. The relative unfavorable orientation of the transforming martensite CVP in the case of compression of the [111] crystal, also explains why the observed hardening is higher under compression versus tension. Since the martensite CVP's are forming through a local shear process, the observed uniaxial hardening is greater, when the plates are oriented less favorably with respect to the loading axis. If the orientation of the martensite plane is accounted for when transforming the local shear stress–strain behavior to the uniaxial stress–strain behavior, the different hardening slopes will be captured.

To further elucidate the above hypothesis, a tensile and compressive stress–strain curve for a NiTi single crystal oriented along the [110] direction is presented in Fig. 4. The [110] orientation is also a primary texture component in the drawn polycrystalline NiTi bar (Fig. 2) and other processed NiTi materials [26]. When a NiTi single crystal is loaded along the [110] direction, the critical transformation stress levels under tension and compression should be similar since the Schmid factors for the transformation are 0.41 and 0.37, respectively [12,35]. Appropriately, the experimentally observed critical transformation stress levels in tension and compression are nearly identical within experimental error (Fig. 4). Furthermore, the transformation stress–strain slopes are comparable under tension and compression (Fig. 4), which is consistent with the equivalent orientations (Schmid factors) of the transforming martensite CVP's. As an aside, the above Schmid factors were derived by assuming that an internally twinned martensite CVP controls the initiation of the stress-induced transformation [12]. Consequently, the consistency with the results in Fig. 4 and the Schmid theory indicate that the formation of an internally twinned CVP governs the critical transformation stress level in NiTi.

Since the Schmid factors under tension versus compression are similar for the [110] orientation, the recoverable strains due to martensite CVP formation are also comparable (5.3 and 4.8%, respectively). However, Fig. 4 demonstrates that the experimentally measured maximum recoverable strains are not equivalent under tension versus compression for the [110] orientation. The difference in the recoverable strain levels for the [110] orientation loaded under tension versus compression is caused by a difference in the attainable detwinning strains under the two stress states. When a NiTi single crystal is loaded along the [110] direction, the crystal is favorably oriented for detwinning under tension (3.3% predicted detwinning strain) but not compression (0.2% predicted detwinning strain) [37]. In summary, the contribution of the martensite detwinning strain is extremely important in the deformation behavior of single crystal and polycrystalline NiTi. Moreover, if the tension-compression asymmetry of the recoverable strain level in of polycrystalline NiTi is to be accurately modeled, the contribution of detwinning strains must be included.

As a final note, some micro-mechanical models assume that the work of the transformation (area under the stress–strain curve) is constant [35,36,38], regardless of the orientation of the test sample or loading direction. We point out that the area under the stress–strain curve is only constant for different orientations and stress states in the *absence of detwinning*. Clearly, Fig. 4 demonstrates that the area under the stress–strain curves is not the same under tension versus compression. If the contribution of detwinning strains is removed from the tensile and compressive stress–strain curves (about 3.3 and 0.2% strain, respectively), then the areas under the tensile and compressive stress–strain curves would be the same.

## 6. Cyclic loading response

The effects of repeated loading cycles on the deformation of single crystal NiTi shape memory alloys is presented in Figs. 5 and 6. The [211] single crystals in Figs. 5 and 6 were aged for a much shorter time compared with the [110] and [111] crystals in Figs. 3 and 4, thus the Ni loss in the matrix was not significant enough to raise the austenite start temperature above room temperature [22,23]. Consequently, the single crystals of the [211] orientation demonstrated pseudoelasticity at room temperature ($T = 295$ K) since their austenite finish temperature was 280 K (Table 1). The [211] single crystals have a tensile Schmid factor of 0.46 and a compressive Schmid factor of 0.39 as calculated using the crystallographic habit plane and transformation direction for CVP formation in NiTi [28,29]. The inverse ratio of the Schmid factors in tension over compression is 0.39/0.46 = 0.85, while the ratio of the critical transformation stress levels in tension over compression is 450/550 MPa = 0.82. Consequently, on the initial loading cycle, the critical transformation stress levels agree with the predictions of Schmid's law within experimental error, which is expected for averaged single crystals [12,22,23].

During cycling, the [211] single crystals demonstrate similar characteristics as polycrystalline NiTi [4,9,13–21]. In general, the critical transformation stress level decreases, the transformation stress–strain slope increases, and the dissipated hysteresis energy decreases (Figs. 5 and 6). The evolution of the stress–strain response in the precipitated single crystals occurs as quickly as demonstrated in earlier polycrystalline studies [18]. Consequently, we believe that grain boundary interactions are not of first order importance during the fatigue of the precipitated NiTi alloys. The interaction between transforming martensite plates and precipitates may control the cyclic deformation and fatigue processes. Recent results on polycrystalline NiTi deformed in the fully martensitic state support the importance of damage induced by intersecting martensite plates [9]. The most intriguing feature in Figs. 5 and 6 is the extremely poor fatigue resistance of the [211] orientation deformed under both tension and compression. Under tension (Fig. 5), numerous samples fractured well below 20 cycles. Under compression (Fig. 6), fracture was not observed, but the samples deformed so dramatically that the characteristic pseudoelastic hysteresis loop became indistinguishable. In the textured polycrystalline NiTi, the [211] orientation demonstrated a below average frequency in the drawing direction. Therefore, drawn and textured polycrystalline may not suffer from the gross deformation characteristics observed in this crystallographic orientation if they are loading along the drawing direction. A large concentration of [211] reflections was found close to the transverse direction. Consequently, the fatigue life in the transverse direction of drawn NiTi polycrystals is expected to be lower than the fatigue life in the drawing direction.

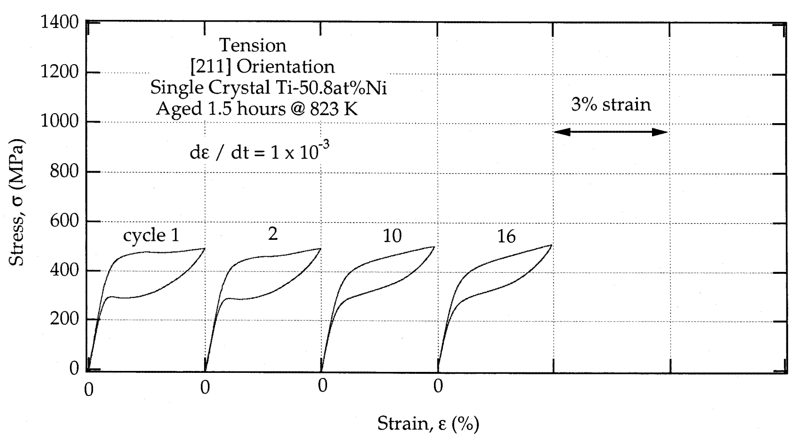


Fig. 5. Tensile cyclic stress–strain response of single crystal NiTi oriented in the [112] direction. The test temperature is above the $A_f$ transformation temperature.

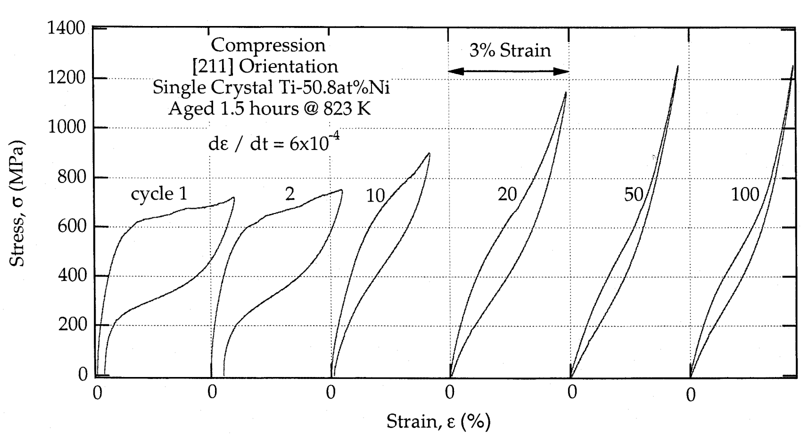


Fig. 6. Compressive cyclic stress–strain response of single crystal NiTi oriented in the [112] direction. The test temperature is above the $A_f$ transformation temperature.

Finally, dislocation motion (slip) has been observed to occur on ⟨010⟩{110} and ⟨010⟩{100} slip systems in the B2 NiTi matrix [40]. When a single crystal of NiTi is loaded along the [211] direction, the [100](011) *slip system* has a Schmid factor of 0.47. Consequently, the [211] orientation is favorably oriented for dislocation motion due to an externally applied tensile or compressive stress. In addition, since the Schmid factors for the *martensitic transformation* are relatively high under both tension and compression (0.46 and 0.39, respectively), the [211] orientation is also favorably oriented for the transformation. In a crystal favorably oriented for the transformation, we assert that martensite interface motion will proceed with little resistance and dislocation generation will be minimized. Given the above observations, the present results indicate that slip caused by external loading may play a strong role in addition to dislocation motion induced by the motion of microscopic martensitic phase boundaries. Earlier studies have normally attributed the buildup of dislocation structures as caused exclusively by the traversing martensite interfaces [9]. Future studies with more orientations of single crystal NiTi are necessary to fully develop our understandings on the fatigue behavior in NiTi. However, the preliminary results presented here show the power of using single crystals to study the cyclic deformation mechanisms in polycrystalline NiTi. In closing we will note that hardening due to latent heat generation [41] may be a factor during cyclic deformation conditions. However, compared with the hardening induced by changes in the microstructure, the contribution due of latent heating is negligible. We assert this since fatigued specimens cooled to room temperature and subsequently cycled demonstrated nearly identical transformation-stress strain slopes as the specimens undergoing back-to-back repeated loading cycles [21].

## 7. Summary

Precipitated single crystal NiTi shape memory alloys demonstrates a strong asymmetry and orientation dependence of mechanical properties, which explains the observed asymmetry in textured polycrystalline NiTi alloys. Consequently, when modeling the cyclic and monotonic behavior of textured polycrystalline NiTi alloys, it is imperative to account for the effects that crystallographic texture has on critical transformation stress levels, martensite plate formation and detwinning strains, and degradation effects during cycling.

## Acknowledgements

The US research is supported by a grant from Department of Energy, Basic Energy Sciences Division, Germantown, Maryland, DOE DEFGO2-93ER14393 and the National Science Foundation, Directorate of Engineering, Mechanics and Materials Program, Arlington, Virginia under grants CMS 94-14525 and CMS 99-00090. The work of Professor Chumlyakov and colleagues is funded by grants from the Russian Fund for Basic Researches, grant # 02-95-00350, MOPO (MGTU, Moscow) and from fund 99-03-32579a.

## References

[1] D.S. Lieberman, M.S. Wechsler, T.A. Read, J. Appl. Phys. 26 (1955) 473.
[2] D.E. Hodgson, M.H. Wu, R.J. Biermann, ASM Handbook 2 (1990) 897.
[3] R.J. Wasilewski, Metall. Mater. Trans. 2 (1971) 2973.
[4] K.N. Melton, O. Mercier, Acta Metall. 27 (1979) 137.
[5] L. Orgeas, D. Favier, J. Phys. IV Colloq. 5 (1995) 605.
[6] K. Jacobus, H. Sehitoglu, M. Balzer, Metall. Mater. Trans. 27A (1996) 3066.
[7] R. Plietsch, K. Fhrlich, Acta Mater. 45 (1997) 2417.
[8] Y. Liu, Z. Xie, J. VanHumbeeck, L. Delaey, Acta Mater. 46 (1998) 4325.
[9] Z. Xie, Y. Liu, J. VanHumbeeck, Acta Mater. 46 (1998) 1989.
[10] L. Orgeas, D. Favier, Acta Mater. 46 (1998) 5579.
[11] K. Gall, H. Sehitoglu, Int. J. Plasticity 15 (1999) 69.
[12] K. Gall, H. Sehitoglu, Y.I. Chumlyakov, I.V. Kireeva, Acta Mater. 47 (1999) 1203.
[13] H. Tamura, K. Mitose, Y. Suzuki, J. de Phys. 5 (1995) C8–617.
[14] M.J. Bigeon, M. Morin, J. de Phys. 5 (1995) C8–385.
[15] T.J. Lim, D.L. McDowell, J. Int. Mater. Sys. Struc. 6 (1995) 817.
[16] B. Stmadel, S. Ohashi, H. Ohtsuka, S. Miyazaki, T. Ishihara, Mater. Sci. Eng. A203 (1995) 187.
[17] B. Strnadel, S. Ohashi, H. Ohtsuka, S. Miyazaki, T. Ishihara, Mater. Sci. Eng. A 202 (1995) 148.
[18] S. Miyazaki, T. Imai, Y. Igo, K. Otsuka, Metall. Mater. Trans. 17A (1986) 115.
[19] H. Tobushi, T. Hachisuka, T. Hashimoto, S. Yamada, J. Eng. Mater. Technol. 120 (1998) 64.
[20] T.J. Lim, D.L. McDowell, J. Eng. Mater. Technol. 121 (1999) 9.
[21] K. Gall, H. Sehitoghi, Y.I. Chumlyakov, I.V. Kireeva, Scr. Met. 40 (1999) 7.
[22] K. Gall, H. Sehitoglu, Y.I. Chumlyakov, I.V. Kireeva, J. Eng. Mater. Technol. 121 (1999) 19.
[23] K. Gall, H. Sehitoglu, Y.I. Chumlyakov, I.V. Kireeva, J. Eng. Mater. Technol. 121 (1999) 28.
[24] K. Gall, H. Sehitoglu, Y.I. Chumlyakov, Y.L. Zuev, I. Karaman, Scr. Met. 39 (1998) 699.
[25] S. Miyazaki, S. Kimura, K. Otsuka, Y. Suzuki, Scr. Met. 18 (1984) 883.
[26] Y.C. Shu, K. Bhattacharya, Acta Mater. 46 (1998) 5457.
[27] Y. Liu, Z. Xie, J. VanHumbeeck, L. Delaey, Acta Mater. 47 (1999) 645.
[28] K.M. Knowles, D.A. Smith, Acta Mater. 29 (1981) 101.
[29] O. Matsumoto, S. Miyazaki, K. Otsuka, H. Tamura, Acta Mater. 35 (1987) 2137.
[30] Q.P. Sun, T.T. Xu, X. Zhang, J. Eng. Mater. Technol. 120 (1999) 38.
[31] M. Nishida, C.M. Wayman, Metallography 21 (1988) 255.
[32] M. Nishida, C.M. Wayman, A. Chiba, Metallography 21 (1988) 255.
[33] S. Miyazaki, K. Otsuka, C.M. Wayman, Acta Mater. 37 (1989) 1873.

[34] S. Miyazaki, K. Otsuka, C.M. Wayman, Acta Mater. 37 (1989) 1885.
[35] T.E. Buchheit, J.A. Wert, Metall. Mater. Trans. 25A (1994) 2383.
[36] T.E. Buchheit, S.L. Kumpf, J.A. Wert, Acta Mater. 43 (1995) 4189.
[37] T.E. Buchheit, J.A. Wert, Metall. Mater. Trans. 27A (1996) 269.
[38] N. Ono, A. Sato, Trans. Jpn. Inst. Metals 29 (1988) 267.
[39] E. Patoor, M. ElAmrani, A. Eberhardt, M. Berveiller, J. de Phys. 5 (1995) C2–495.
[40] Y.I. Chumlyakov, N.S. Surikova, A.D. Korotaev, Phys. Met. Metall. 82 (1996) 102.
[41] J. Shaw, S. Kyriakides, Acta Metall. 45 (1997) 683.